Available online at www.sciencedirect.com
ScienceDirect
Ceramics International 34 (2008) 1595–1602
CERAMICS INTERNATIONAL
www.elsevier.com/locate/ceramint

Microstructure refinement of alumina Optimisation by gas pressure sintering process

C. Nivot, F. Valdivieso *

Département Céramiques Spéciales, Centre SMS, UMR CNRS 5146, Ecole Nationale Supérieure des Mines de Saint-Etienne, 158 cours Fauriel, 42023 Saint-Etienne Cedex 2, France

Received 12 March 2007; received in revised form 6 April 2007; accepted 2 May 2007
Available online 2 June 2007

Abstract

This paper investigates densification and grain growth evolutions during gas pressure sintering of alumina. Isothermal sintering runs are performed under different nitrogen pressures: atmospheric pressure and 2 MPa. Experimental data are fitted thanks to constitutive laws in order to understand nitrogen pressure effect on densification and grain growth mechanisms of a fine-grained alumina. An optimal run of densification is proposed as an application of these results.

Keywords: A. Sintering; A. Grain growth; D. Al_2O_3; Gas pressure sintering

1. Introduction

In a previous work [1], we studied an insoluble gas (nitrogen) pressure effect on non-isothermal alumina sintering. It mainly attempted to characterize the nitrogen pressure effect on non-densifying mechanisms. This paper is focused on nitrogen pressure effect on a fine-grained alumina densification and grain growth mechanisms. Young and Cutler [2] proposed expressions which link size variation of sample during non-isothermal sintering with diffusional mechanism which governs densification: grain boundary diffusion or volume diffusion and/or by lattice diffusion. Wang and Raj [3] performed activation energy calculation from results obtained by dilatometric measurements with different heating rates. Recently, Fang et al. [4] showed that dilatometric results obtained during non-isothermal sintering runs are not suitable to determine activation energy because of depending on the heating rate. Cocks and coworkers [5–11] used isothermal sintering runs in order to determine mechanism densification. They proposed that grain boundary diffusion or interface reaction is the dominant mechanism. Model equations are expressed as a function of two measurable and comparable physical quantities: relative density and grain size. Moreover, densification rate and grain growth rate depend on the sintering stage: open porosity domain and closed porosity domain. Although it is established [3,12–15] that alumina densification is controlled by grain boundary diffusion, authors [10,11,16] showed that interface reaction can control the densification. He and Ma [17,18] applied these models in the case of alumina sintering. They calculated densification activation energy and showed that interface reaction at grain boundaries limits densification in the intermediate stage of sintering.

The purpose of this work is to characterize the nitrogen pressure effect on alumina densification mechanisms and to determine the activation energy value by means of model developed by Cocks et al. The use of this model involves relative density and grain size characterizations. Experimental conditions are deduced from a previous work [1] so the nitrogen pressure influence on isothermal alumina sintering will be focused on the differences on densification and microstructure between atmospheric pressure and 2 MPa. Kang and Yoon [19] showed that a pore which contains insoluble gas under pressure cannot reduce its size below critical size. Thus sintering runs under pressure have been performed up to temperature for which porosity is still open ($T \leq 1500\ ^\circ C$).

* Corresponding author. Tel.: +33 477 420 083; fax: +33 477 420 249.
E-mail address: francois.valdivieso@emse.fr (F. Valdivieso).

0272-8842/$34.00
doi:10.1016/j.ceramint.2007.05.002

2. Experimental procedure

2.1. Green compacts

A spray-dried pure (99.98%) alumina powder (Baikowski Chimie, France) of 0.2 μm average particle size with 500 ppm of MgO as doping element was used. Green compacts were prepared by uniaxial pressing under 150 MPa in order to form pellets of 13 mm diameter. The green compact density was 52 ± 1% of the theoretical value (3.987 g/cm^3).

2.2. Sintering run

Densification was performed by gas pressure sintering (GPS) in a graphite resistance heated furnace (KCE FPW100/150-2200-100-AS).

The typical isothermal sintering run involves: (1) pressurization with N_2 gas to the desired pressure (0.1 or 2 MPa) at room temperature, (2) heating to the selected temperature (between 1350 and 1500 °C) at a rate of 5 °C/min, (3) holding at the fixed temperature for 0 and 120 min, (3) depressurization of the system in 2 min as soon as the holding is ended and (4) cooling to room temperature at a rate of about 40 °C/min. It must be underlined that samples are neither encapsulated nor introduced in an alumina powder bed. Green compacts are put in the furnace and they are only under hydrostatic gas pressure, without any external mechanical force.

2.3. Characterizations

Final relative density was measured by using the water-immersion method. Microstructures were observed by field emission scanning electron microscopy (Model 6500F, JEOL, Japan) on polished surfaces and then thermally etched during 30 min at $T = T_{\text{sintering}} - 50$ °C. Average grain sizes were obtained by the intercept method on micrographs and statistical diameter distributions were determined by use of image analyser software (Analysis).

3. Results

3.1. Results on densification

Relative density evolution of alumina samples during isothermal sintering under nitrogen pressure is represented in Fig. 1.

This figure shows that a holding at temperature allows to improve densification whatever the nitrogen pressure applied. However, results on materials sintered at lowest temperatures under 2 MPa are still lower than results obtained on atmospheric nitrogen pressure sintered materials. At 1350 and 1425 °C, the relative density obtained under nitrogen pressure is always lower than those obtained at atmospheric pressure. At 1500 °C after 30 min under pressure, relative densities are close to those obtained under atmospheric pressure (indeed, the relative density reduction under pressure is 1%).

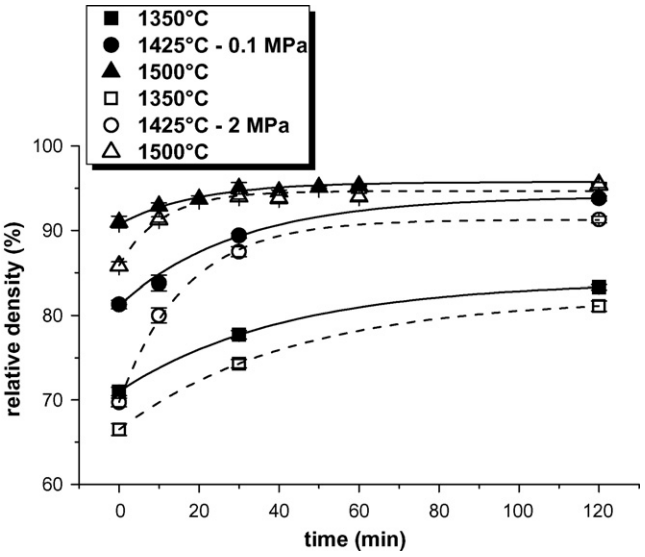

Fig. 1. Relative density of materials sintered at different temperatures under nitrogen pressures of 0.1 and 2 MPa vs. sintering time.

3.2. Results on microstructure

Fig. 2 represents average grain size evolution versus time at the considered temperatures and pressures. Nitrogen pressure has no significant influence at 1350 °C, however the reduction of the average grain size is about 5% at 1425 °C and 20% at 1500 °C. Fig. 3 represents grain diameter distributions for materials sintered at 1500 °C under 0.1 and 2 MPa for a holding of 30 min (a), 60 min (b) and 120 min (c). For materials sintered under 2 MPa, whatever the holding duration, the mode of the distribution is shifted towards smallest average diameters and it must be noticed that pressure reduces distribution width.

Non-isothermal alumina sintering under nitrogen pressure underlined the importance of sintering trajectory representation proposed by Kanters et al. [20]. The sintering trajectory, which

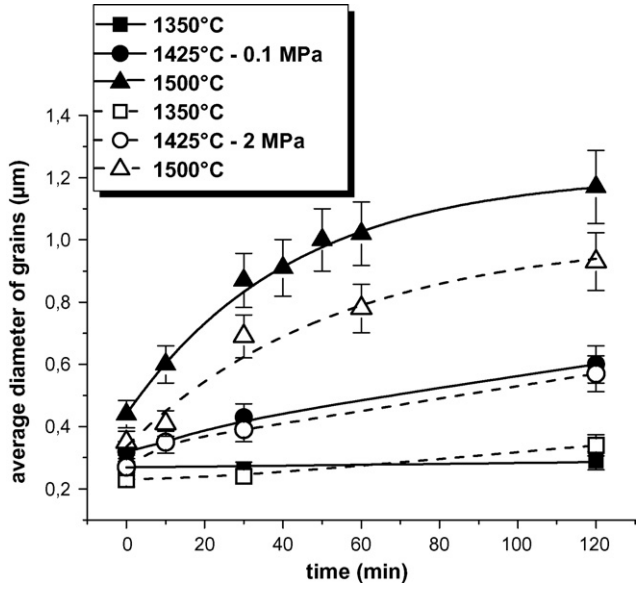

Fig. 2. Average grain size as a function of sintering time.

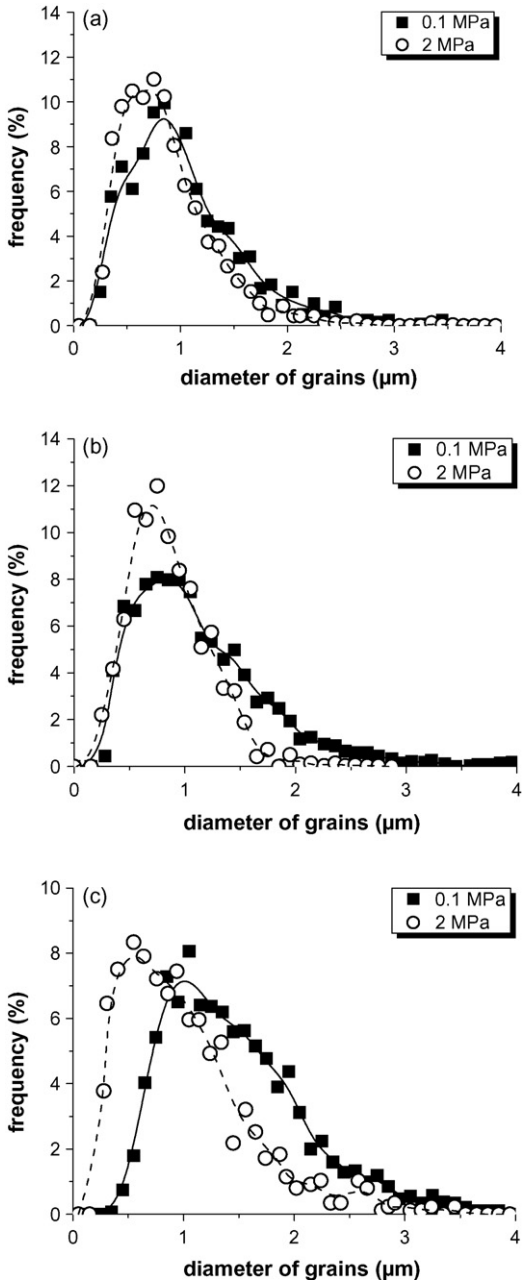

Fig. 3. Grain diameter distributions of materials sintered at 1500 °C during (a) 30 min, (b) 60 min and (c) 120 min.

is defined as the average grain size versus relative density, is represented in Fig. 4. This figure shows that grain growth evolution is the same one whatever the nitrogen pressure applied during isothermal sintering run (0.1 or 2 MPa). Sintering trajectories representation shows that fine-grained alumina grain growth law is not influenced by nitrogen under pressure even during isothermal runs up to a relative density of 95%.

4. Discussion

The aim of the part below is the experimental results interpretation in order to determine densification and grain growth mechanisms thanks to models developed in the literature.

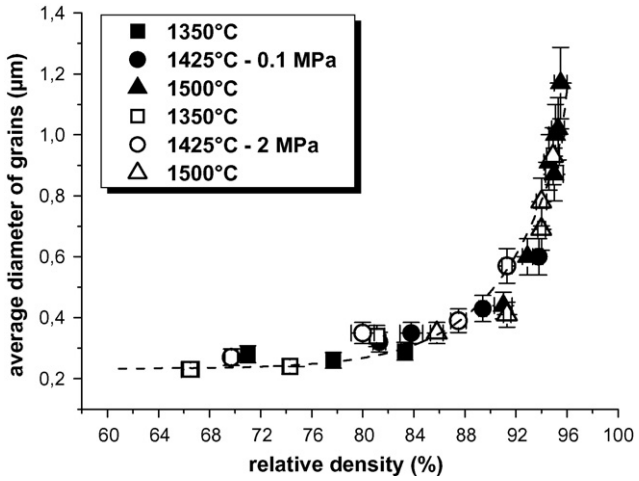

Fig. 4. Sintering trajectory of alumina samples isothermally sintered under nitrogen pressures: 0.1 and 2 MPa.

4.1. Constitutive laws

Micromechanical models developed by Cocks and co-workers [5–11] are established for each stage of sintering in order to predict the shape change, development of stress field and microstructure evolution during hot isostatically pressed materials. Sintering process is divided into two stages. In the early stage of densification, pores are connected, discrete necks exist between particles and the relative density of materials is less than 0.9: this stage is called stage 1. With the increase in time, the pores become isolated: stage 2 begins. The transition between stage 1 and stage 2 occurs for relative density of materials typically included between 0.9 and 0.95.

4.1.1. Boundary diffusion controlled densification

If grain boundary diffusion controls densification, during stage 1 and stage 2 the densification rate, $\dot{\rho}$ during sintering can be written as

$$\dot{\rho} = 9\rho\dot{\varepsilon}_{0b}\left(\frac{L_0}{L}\right)^3 f_b(\rho)\left(\frac{\sigma_s}{\sigma_0}\right) \quad (1)$$

where $\dot{\varepsilon}_{0b}$ is the uniaxial strain rate under an applied stress σ_0 (defined by Eq. (2)) for a material of initial grain size L_0 and L is the grain size:

$$\sigma_0 = \frac{\gamma}{L_0} \quad (2)$$

with γ superficial energy equal to 1 J m^{-2} [18].

Sintering stress σ_s expressions are given for stage 1 and stage 2 of sintering by Eqs. (3) and (4), respectively:

$$\sigma_s = \frac{\gamma}{0.06L}\rho^2(2\rho - \rho_0) \quad (3)$$

$$\sigma_s = \frac{4\gamma}{L}\left(\frac{1-\rho}{6}\right)^{-1/3} \quad (4)$$

where ρ is the relative density and ρ_0 is the initial relative density.

$f_b(\rho)$ expressions are given for stage 1 and stage 2 of sintering by Eqs. (5) and (6), respectively:

$$f_b(\rho) = 0.54\frac{(1-\rho_0)^2}{\rho(\rho-\rho_0)^2} \tag{5}$$

$$f_b(\rho) = 3.2\frac{(1-\rho)^{1/2}}{\rho} \tag{6}$$

4.1.2. Interface reaction controlled densification

For stage 1 of sintering, if interface reaction controls densification the densification rate expression $\dot{\rho}$ is obtained by

$$\dot{\rho} = 27\rho\dot{\varepsilon}_{0r}\left(\frac{L_0}{L}\right) f_r^2(\rho)\left(\frac{\sigma_s}{\sigma_0}\right)^2 \tag{7}$$

with

$$f_r(\rho) = \frac{1}{3}\frac{(1-\rho_0)}{\rho^{3/2}\rho_0^{1/2}(\rho-\rho_0)} \tag{8}$$

For stage 2 of sintering, if interface reaction controls densification, the densification rate expression is

$$\dot{\rho} = 27\rho\dot{\varepsilon}_{0r}\left(\frac{L_0}{L}\right) f_r^{6/5}(\rho)\left(\frac{\sigma_s}{\sigma_0}\right)^2 \tag{9}$$

with

$$f_r(\rho) = \frac{0.042}{[1-1.53(1-\rho)^{2/3}]^{5/3}} \tag{10}$$

4.1.3. Grain growth modelling

Grain growth activation energy calculation is based on the model proposed by Du and Cocks [11] and applied by He and Ma [17,18] in case of free sintering. Grain growth rate controlled by surface diffusion, $\dot{L} = f(\rho, L, T)$, depends on material densification state. Parameters which determine densification state of material are relative density ρ, grain size L and sintering temperature T. Grain growth rate expressions are given by Eqs. (11) and (12) for, respectively, stage 1 and stage 2 of sintering:

$$\dot{L} = \dot{L}_0\left(\frac{L_0}{L}\right)^3(1-\rho)^{-3/2} \tag{11}$$

$$\dot{L} = \dot{L}_0\left(\frac{L_0}{L}\right)^3(1-\rho)^{-4/3} \tag{12}$$

where L_0 is the initial grain size and $\dot{L}_0$ is a grain growth rate constant which is linked to sintering temperature T. As for densification activation energy calculation, grain growth activation energy Q_g is deduced from $\dot{L}_0$ expression:

$$\dot{L}_0 = \frac{\dot{L}_{00}}{T}\exp\left(\frac{-Q_g}{RT}\right) \tag{13}$$

where $\dot{L}_{00}$ is a material constant independent of temperature and Q_g the activation energy for grain growth controlled by surface diffusion.

4.2. Analysis

4.2.1. Densification

Densification rate $\dot{\rho}$ is expressed as a function of one of both possible limiting mechanisms. Thus, experimental results are modelled by considering grain boundary diffusion (identified as GB control) and interface reaction (identified as IR control) as limiting densification mechanism for each sintering temperature: 1350, 1425 and 1500 °C. Moreover, densification rate expressions are defined for each stage of sintering: stage 1 (pores are interconnected) and stage 2 (pores are closed). According to Du and Cocks, the transition between stage 1 and stage 2 occurs for a relative density of 0.9–0.95. Fig. 1 shows that we can consider materials sintered at 1350 and 1425 °C as materials in stage 1 of sintering for the two nitrogen pressures studied. Results obtained on materials isothermally sintered at 1500 °C under 0.1 and 2 MPa show that most of those samples present closed porosity: they are in stage 2 of sintering.

Fig. 5 represents densification modelling of a fine-grained alumina (L_0 = 0.2 μm) sintered under nitrogen pressure. Green compact relative density ρ_0 is taken equal to 0.52. $\dot{\varepsilon}_{0b}$ and $\dot{\varepsilon}_{0r}$ are determined by fitting of the constitutive model to the experimental data. These figures show that modelling which

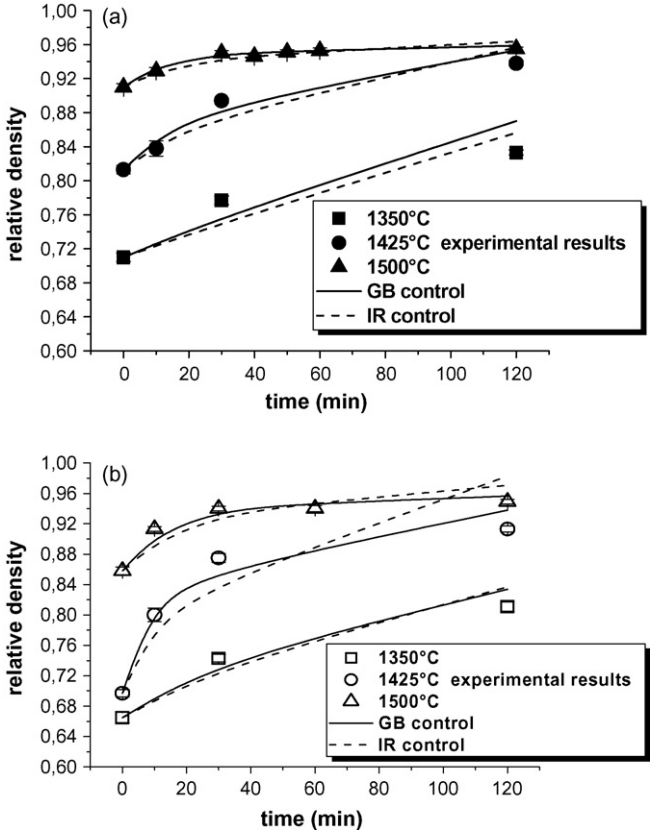

Fig. 5. Modelling of densification at 1350, 1425 and 1500 °C under (a) 0.1 MPa and (b) 2 MPa.

considers grain boundary diffusion as limiting densification mechanism proposes the best experimental results fit, contrary to He and Ma [17,18] who showed that interface reaction is the limiting densification mechanism of alumina with initial grain size of 0.9 μm. In addition, limiting densification mechanism can be confirmed by $(\ln(\mathrm{d}\rho/\mathrm{d}t))_T = f(\ln r)$ plot. Indeed, the densification rate $\mathrm{d}\rho/\mathrm{d}t$ can be linked with the average grain size r by the following equation:

$$\frac{1}{\rho}\frac{\mathrm{d}\rho}{\mathrm{d}t} = K\frac{D\gamma\Omega}{\rho r^n RT} \tag{14}$$

where n depends on mechanism of densification ($n = 3$ or 4 for respectively volume and grain boundary diffusion) and where ρ is the relative density, K a proportionality coefficient, D a diffusion coefficient, γ the surface energy and Ω is the molar volume of the material.

Fig. 6 represents $(\ln(\mathrm{d}\rho/\mathrm{d}t))_T = f(\ln r)$ for the sintering temperatures and nitrogen pressures studied; slope (n) and regression coefficient values are summarized in Table 1. Linear regression of experimental results shows that slope values are close to −4 and regression coefficient values are almost higher than 0.9, which highlights a good agreement with the equation of densification controlled by grain boundary diffusion. Thus, results deduced from micro-mechanical modelling proposed by Cocks and co-workers show that the alumina sintering under nitrogen pressure is controlled by grain boundary diffusion whatever the nitrogen pressure applied: 0.1 or 2 MPa.

Considering grain boundary diffusion as the main mechanism responsible of alumina densification during sintering under nitrogen pressures of 0.1 and 2 MPa, densification activation energy is calculated by $\dot{\varepsilon}_{0b} = (\dot{\varepsilon}_{00b}/T)\exp(-Q_{db}/RT)$ proposed by He and Ma [18]. Activation energy value deduced from slopes is 517 ± 17 kJ mol^{-1} whatever the nitrogen pressure applied (Fig. 7). The value is in agreement with those found in the literature [2–4,22,23]. Considering incertitude linked to $\dot{\varepsilon}_{0b}$ determination, we can conclude that alumina densification controlled by grain boundary diffusion is not influenced by the presence of nitrogen under pressure in the domain of relative densities considered. But, for a considered temperature, the densification rate under atmospheric pressure is higher than the one under 2 MPa.

Table 1
Slope and regression coefficient values from Fig. 6

Sintering conditions		Slope	Regression coefficient
1350 °C	0.1 MPa	−3.49	0.87
	2 MPa	−3.52	0.97
1425 °C	0.1 MPa	−3.74	0.94
	2 MPa	−3.59	0.93
1500 °C	0.1 MPa	−3.91	0.95
	2 MPa	−3.72	0.94

4.2.2. Grain growth activation energy

Grain growth activation energy determination is based on surface diffusion model proposed by Du and Cocks [11]. Grain growth rate, $\dot{L}$, is calculated with an initial grain size $L_0 = 0.2$ μm thanks to Eq. (11) in order to model grain growth of materials sintered at 1350 and 1425 °C and, thanks to Eq. (12) for the grain growth modelling of materials sintered at 1500 °C. Modelling results are represented in Fig. 8. Curves which represent model on these graphs are obtained by grain growth rate constant ($\dot{L}_0$) adjustment in order to fit the experimental data, which are also reported on these graphs. These figures show a good adequacy between experimental results and model, which supposes that the grain growth was controlled by surface diffusion. Whatever the nitrogen pressure applied during isothermal sintering of a fine-grained alumina, the grain growth controlled by surface diffusion model is verified. Same results are obtained by He and Ma [17,18] on alumina slightly coarser than that of this work.

Since grain growth modelling considering a process controlled by surface diffusion is verified, grain growth activation energy can be determined from $\ln(T\dot{L}_0) = f(1/T)$ plot (Fig. 9) as expressed by Eq. (13). The linear regression of experimental results obtained on materials sintered under atmospheric nitrogen pressure gives grain growth activation

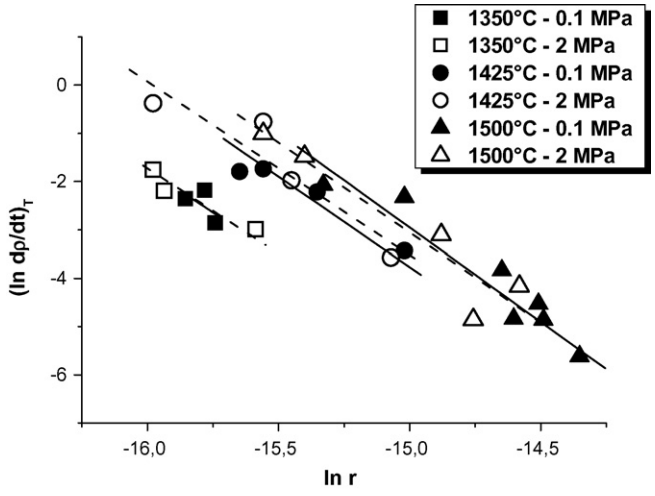

Fig. 6. $(\ln(\mathrm{d}\rho/\mathrm{d}t))_T = f(\ln r)$ for different isothermal sintering conditions.

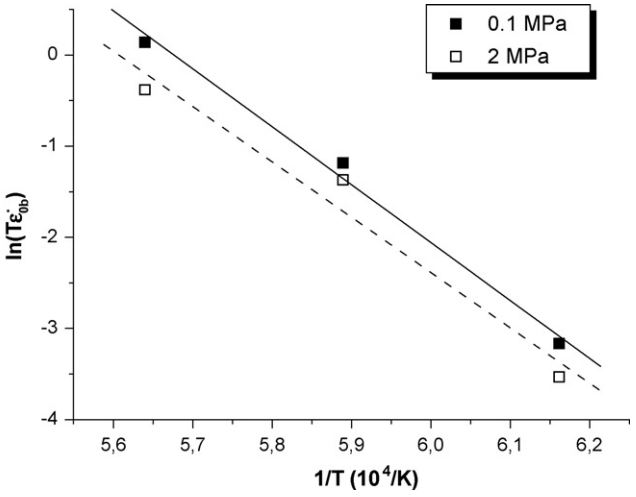

Fig. 7. $\ln(T\dot{\varepsilon}_{0b}) = f(1/T)$ for sintering runs under 0.1 and 2 MPa.

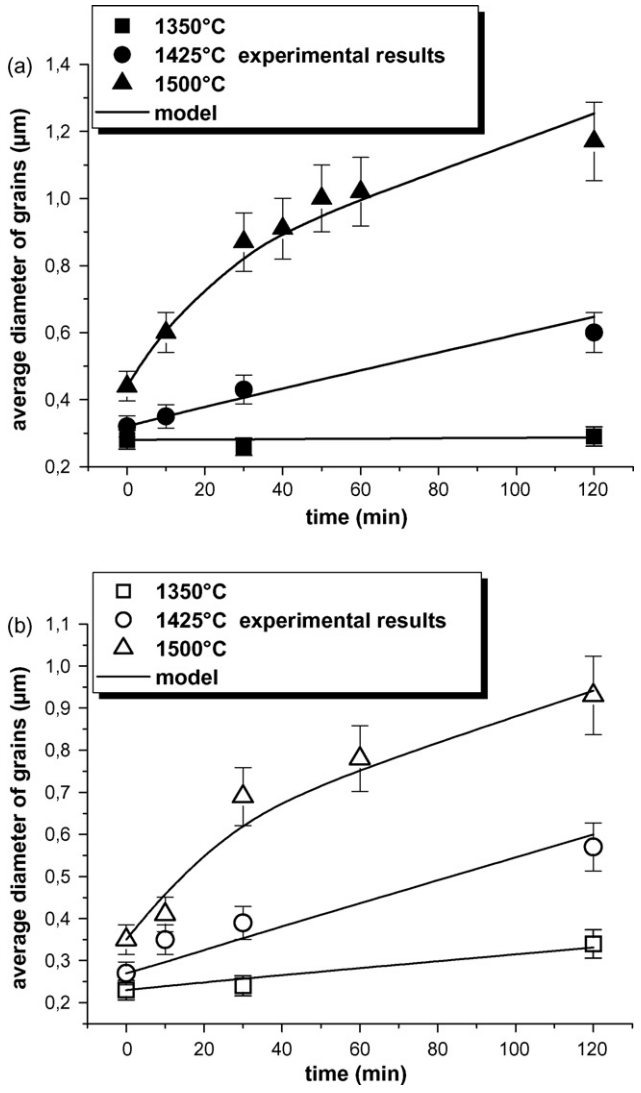

Fig. 8. Modelling of grain growth at 1350, 1425 and 1500 °C under (a) 0.1 MPa and (b) 2 MPa.

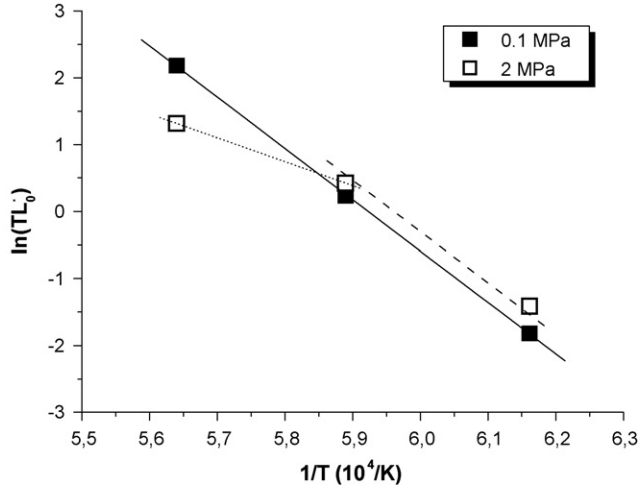

Fig. 9. $\ln(T\dot{L}_0) = f(1/T)$ for sintering runs under 0.1 and 2 MPa.

energy of 638 kJ mol^{-1} for a regression coefficient which is 0.99. This result is slightly higher than those of the literature: 476 kJ mol^{-1} [17] and 500 kJ mol^{-1} [21].

Concerning the interpretation of results obtained on materials sintered under 2 MPa, linear regression of the three experimental results gives grain growth activation energy of 437 kJ mol^{-1}. This activation energy value is quite lower than that obtained on materials sintered under 0.1 MPa. This low value of energy would indicate that, for a given sintering temperature, grain growth would be favoured for materials sintered under 2 MPa. However this conclusion is not in agreement with results in Fig. 2 which shows, for a given sintering temperature, a reduction of the average grain diameter of materials sintered under 2 MPa compared to materials sintered under nitrogen atmospheric pressure.

But we could think that it's more suitable to consider two slopes as shown in the graph. At lower temperatures a unique value of grain growth activation energy exists in the intermediate stage of sintering whatever the nitrogen pressure applied. The change of slope imposed by the point corresponding to the sintering at 1500 °C induces that grain growth is limited by another mechanism, which takes into account mobility of pores containing gas under pressure since at this temperature, porosity closure occurs during the stage.

5. Application for optimal microstructure

During intermediate stage of the sintering (open porosity domain), nitrogen pressure has no significant effect on densification and grain growth mechanisms. But densification rate and grain size are lower under pressure than under atmospheric pressure. With these considerations, we can affirm that materials sintered under nitrogen pressure can reach the end of the intermediate stage of sintering (just before pore closure) with a finer microstructure than materials sintered under atmospheric pressure. Moreover the pore closure occurs at higher temperature under 2 MPa than under 0.1 MPa. The next section of this paper is devoted to the study of depressurisation effect on densification and microstructure of alumina samples.

5.1. Experimental process

The samples are maintained under pressure (2 MPa) during the ramp of temperature up to 1500 °C to keep an open porosity. Then the nitrogen pressure is released with different rates (in 2, 10, 20 and 30 min) at 1500 °C. And a holding time of 30 min at atmospheric pressure is required before the temperature decrease to room temperature in order to continue densification (this cycle is identified as C2).

5.2. Results

Fig. 10 represents relative densities versus the total holding time at 1500 °C for materials isothermally sintered under nitrogen atmospheric pressure and materials sintered with a pressure release as described above. This figure shows that

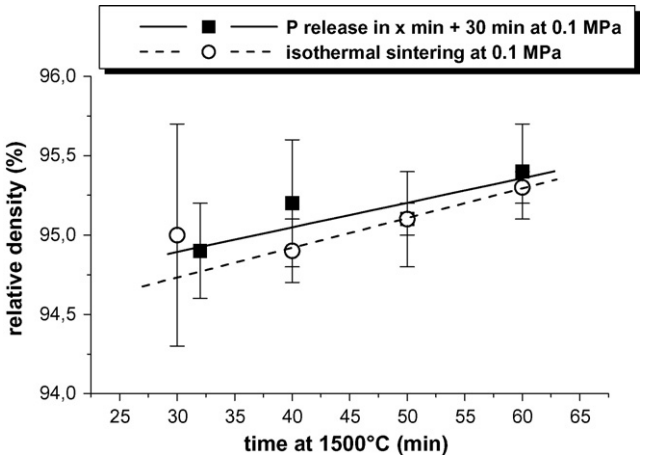

Fig. 10. Relative density evolution vs. time of alumina samples sintered in different nitrogen pressure conditions.

sintering run with depressurisation is able to slightly improve densification of alumina samples compared with isothermally sintered ones for a given duration at 1500 °C.

Sintering trajectories of materials sintered during these different heating runs are represented in Fig. 11. It illustrates that heating under nitrogen pressure followed with depressurisation modifies the sintering trajectory. Indeed for a given relative density, material sintered during the cycle C2 presents average grain size which is 15% lower than isothermal sintered material.

5.3. Interpretation

Du and Cocks [11] proposed to calculate the sintering stress σ_s for a sample with closed porosity from the formula given by Eq. (4). Fig. 12 which represents sintering stresses σ_s calculated for studied materials highlights higher sintering stresses for materials sintered under C2 conditions than isothermal sintered ones. So we can explain the sintering trajectory modification

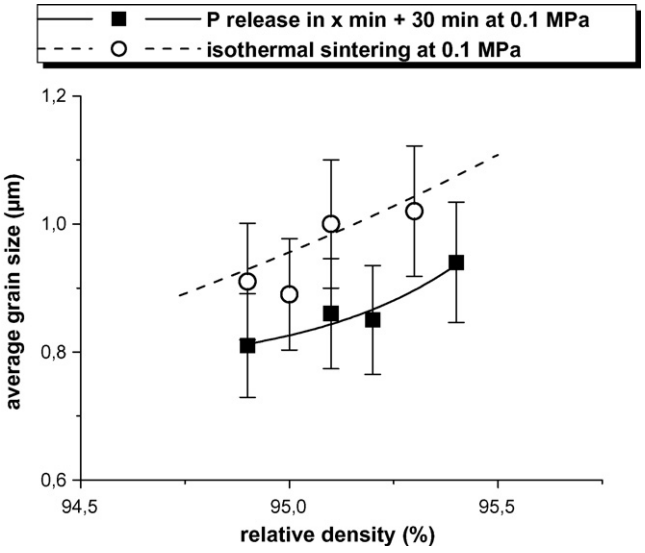

Fig. 11. Influence of nitrogen pressure release on sintering trajectory.

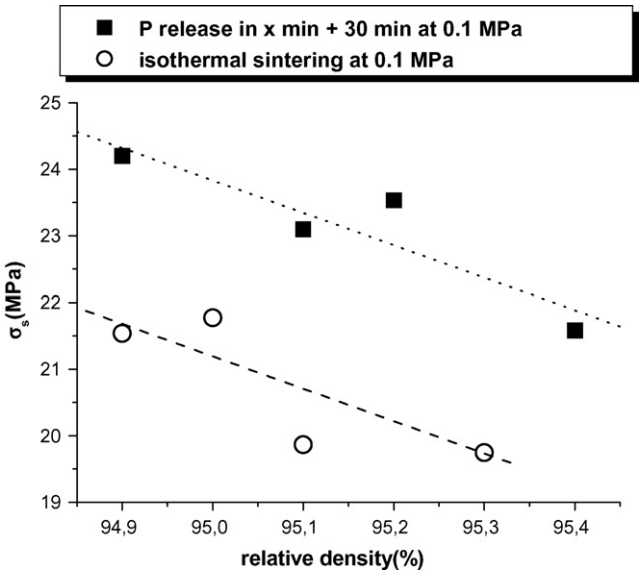

Fig. 12. Sintering stress for different sintering runs.

thanks to this higher sintering stress value. Indeed temperature increase up to 1500 °C under nitrogen pressure maintains finer microstructure, which confers high sinterability to these materials when depressurisation occurs. Thus, compared with isothermal sintering run under 0.1 MPa nitrogen, this sintering run permits to keep finer and more homogeneous microstructure with a slight increase of relative density.

6. Conclusion

Densification and grain growth activation energies are deduced from models developed in the literature. In the intermediate stage of sintering, the gas pressure does not have any effect on densification and grain growth mechanisms but their kinetics are modified. It is possible to use this property to obtain a finer microstructure for a slight increase of relative density. Indeed this study showed that a temperature increase under nitrogen pressure followed by a depressurization and a stage under atmospheric pressure is able to improve densification and decrease grain size compared with an isothermal sintering run under nitrogen atmospheric pressure.

References

[1] C. Nivot, F. Valdivieso, P. Goeuriot, Nitrogen pressure effect on non-isothermal alumina sintering, J. Eur. Ceram. Soc. 26 (1–2) (2006) 9–15.
[2] W.S. Young, I.B. Cutler, Initial sintering with constant rates of heating, J. Am. Ceram. Soc. 53 (12) (1970) 659–663.
[3] J. Wang, R. Raj, Estimate of the activation energies for boundary diffusion from rate-controlled sintering of pure alumina, and alumina doped with zirconia and titania, J. Am. Ceram. Soc. 73 (5) (1990) 1172–1175.
[4] T.-T. Fang, J.-T. Shiue, F.-S. Shiau, On the evaluation of the activation energy of sintering, Mater. Chem. Phys. 80 (2003) 108–113.
[5] Z.Z. Du, A.C.F. Cocks, Constitutive models for the sintering of ceramic components. I. Material models, Acta Metall. Mater. 40 (8) (1992) 1969–1979.
[6] Z.Z. Du, A.C.F. Cocks, Constitutive models for the sintering of ceramic components. II. Sintering of inhomogeneous bodies, Acta Metall. Mater. 40 (8) (1992) 1981–1994.

[7] A.C.F. Cocks, Z.Z. Du, Pressureless sintering and hipping of inhomogeneous ceramic compacts, Acta Metall. Mater. 41 (7) (1993) 2113–2126.
[8] J. Pan, A.C.F. Cocks, A constitutive model for stage 2 sintering of fine grained materials. I. Grain-boundaries act as perfect sources and sinks for vacancies, Acta Metall. Mater. 42 (4) (1994) 1215–1222.
[9] J. Pan, A.C.F. Cocks, A constitutive model for stage 2 sintering of fine grained materials. II. Effects of an interface reaction, Acta Metall. Mater. 42 (4) (1994) 1223–1230.
[10] A.C.F. Cocks, The structure of constitutive laws for the sintering of fine grained materials, Acta Metall. Mater. 42 (7) (1994) 2191–2210.
[11] Z.Z. Du, A.C.F. Cocks, Sintering of fine-grained materials by interface reaction controlled grain boundary diffusion, Int. J. Solids Struct. 31 (10) (1994) 1429–1445.
[12] E. Arzt, M.F. Ashby, K.E. Easterling, Practical applications of hot-isostatic pressing diagrams: four case studies, Metall. Trans. A 14 (1983) 211–221.
[13] A.S. Helle, K.E. Easterling, M.F. Ashby, Hot isostatic diagrams: new developments, Acta Metall. Mater. 33 (12) (1985) 2163–2174.
[14] J.G. Li, X. Sun, Synthesis and sintering behavior of nanocrystalline alpha alumina powder, Acta Mater. 48 (2000) 3103–3112.
[15] W. Zeng, L. Gao, L. Gui, J. Guo, Sintering kinetics of alpha Al_2O_3 powder, Ceram. Int. 25 (1999) 723–726.
[16] J. Besson, M. Abouaf, Rheology of porous alumina and simulation of hot isostatic pressing, J. Am. Ceram. Soc. 75 (8) (1992) 2165–2172.
[17] Z. He, J. Ma, Densification and grain growth during interface reaction controlled sintering of alumina ceramics, Ceram. Int. 27 (2001) 261–264.
[18] Z. He, J. Ma, Constitutive modelling of the densification and grain growth of fine grained alumina ceramics, Mater. Sci. Eng. A 361 (2003) 130–135.
[19] S.-J.L. Kang, K.J. Yoon, Densification of ceramics containing entrapped gases, J. Eur. Ceram. Soc. 5 (1989) 135–139.
[20] J. Kanters, U. Eisele, J. Rödel, Effect of initial grain size on sintering trajectories, Acta Mater. 48 (2000) 1239–1246.
[21] H.J. Frost, M.F. Ashby, Deformation Mechanism Maps, Pergamon Press, Oxford, 1982.
[22] G.L. Messing, M. Kumagai, Low-temperature sintering of α-alumina-seeded boehmite gels, Am. Ceram. Soc. Bull. 73 (10) (1994) 88–91.
[23] E. Sato, C. Carry, Effect of powder granulometry and pre-treatment on sintering behavior of submicron-grained α-alumina, J. Eur. Ceram. Soc. 15 (1995) 9–16.